# COUPLING OF SINGLE-MODE OPTICAL FIBERS TO GaAs WAVEGUIDES

WASHINGTON UNIVERSITY
ST. LOUIS, MISSOURI

OCTOBER 1976

RADC-TR-76-313
Interim Technical Report #1
October, 1976

# COUPLING OF SINGLE-MODE OPTICAL FIBERS TO GaAs WAVEGUIDES

Washington University
Laboratory for Applied Electronic Sciences

Approved for public release; distribution unlimited

Sponsored by

Defense Advanced Research Projects Agency
ARPA Order No. 3020



ROME AIR DEVELOPMENT CENTER
AIR FORCE SYSTEMS COMMAND
GRIFFISS AIR FORCE BASE, NEW YORK 13441

This report has been reviewed by the RADC Information Office (OI) and is releasable to the National Technical Information Service (NTIS). At NTIS it will be releasable to the general public, including foreign nations.

This technical report has been reviewed and is approved.

ANDREW C. YANG
Contract Monitor

Unclassified

SECURITY CLASSIFICATION OF THIS PAGE *(When Data Entered)*

| REPORT DOCUMENTATION PAGE | | READ INSTRUCTIONS BEFORE COMPLETING FORM |
|---|---|---|
| 1. REPORT NUMBER<br>RADC-TR-76- 313 | 2. GOVT ACCESSION NO. | 3. RECIPIENT'S CATALOG NUMBER |
| 4. TITLE *(and Subtitle)*<br>COUPLING OF SINGLE-MODE OPTICAL FIBERS TO GaAs WAVEGUIDES | | 5. TYPE OF REPORT & PERIOD COVERED<br>Interim<br>1 Aug 75 to 31 Jan 76<br>6. PERFORMING ORG. REPORT NUMBER<br>Semiannual Tech Rpt No. 1 |
| 7. AUTHOR(s)<br>William S. C. Chang | | 8. CONTRACT OR GRANT NUMBER(s)<br>F19628-76-C-0032 |
| 9. PERFORMING ORGANIZATION NAME AND ADDRESS<br>Washington Univ<br>Applied Electronic Sciences Laboratory, Box 1115<br>St. Louis, Missouri 63130 | | 10. PROGRAM ELEMENT, PROJECT, TASK AREA & WORK UNIT NUMBERS<br>PE 61101E<br>ARPA Order No. 3020 |
| 11. CONTROLLING OFFICE NAME AND ADDRESS<br>Defense Advanced Research Projects Agency<br>1400 Wilson Blvd. Arlington, VA 22209 | | 12. REPORT DATE<br>October 1976<br>13. NUMBER OF PAGES<br>42 |
| 14. MONITORING AGENCY NAME & ADDRESS *(if different from Controlling Office)*<br>Deputy for Electronic Technology (RADC/ETSD)<br>Hanscom AFB, MA 01731<br>Monitor/Andrew Yang/ETSD | | 15. SECURITY CLASS. *(of this report)*<br>Unclassified<br>15a. DECLASSIFICATION/DOWNGRADING SCHEDULE |

16. DISTRIBUTION STATEMENT *(of this Report)*

Approved for public release; distribution unlimited

17. DISTRIBUTION STATEMENT *(of the abstract entered in Block 20, if different from Report)*

18. SUPPLEMENTARY NOTES

This research is sponsored by the Defense Advanced Research Projects Agency
ARPA Order No. 3020

19. KEY WORDS *(Continue on reverse side if necessary and identify by block number)*

Integrated optics
Thin film waveguides
Fiber to waveguide coupler
Transitional waveguide
GaAs waveguides

20. ABSTRACT *(Continue on reverse side if necessary and identify by block number)*

An investigation was conducted to find an efficient method to couple a single-mode optical fiber to a GaAs waveguide at near infrared wave lengths. The general approach is to first fabricate a transitional waveguide. The fiber and the transitional waveguide are then coupled together by the tapered velocity coupling method. Step index transitional waveguide structures were fabricated and evaluated with a coupling efficiency of 77%, a value close to theoretical limit. Fabrication of silica fiber horn was not successful due to the thermal

DD FORM 1 JAN 73 1473 EDITION OF 1 NOV 65 IS OBSOLETE

Unclassified

SECURITY CLASSIFICATION OF THIS PAGE *(When Data Entered)*

properties of the silica fiber materials. Alternative methods are being investigated to match the cylindrical geometry of the fiber to the planar geometry of the uniform waveguide, replacing the fiber horn.

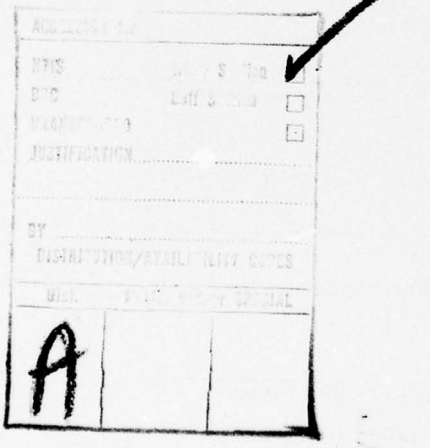

## 1. SUMMARY

The object of this research contract is to find an efficient method to couple a single-mode optical fiber to a GaAs waveguide at near infrared wavelengths. The general approach is to first fabricate a transitional waveguide. The fiber and the transitional waveguide are then coupled together by the tapered velocity coupling method.

During this reporting period, the following research work has been undertaken:

- Fabrication and evaluation of the step index transitional waveguide structure as discussed in the original proposal. A coupling efficiency of 77 percent has been achieved, a value close to the theoretical limit.
- Invention of a new transitional waveguide structure. This structure utilizes a "hollow" dielectric waveguide on top of a GaAs substrate.
- Fabrication and evaluation of a silica fiber horn. Our investigation indicates that this method will not succeed because of the thermal properties of the silica fiber materials. On the other hand, if single-mode glass fibers can be developed in the future, the fiber horn may still be an attractive approach.
- Fabrication and evaluation of transitional structures on low index films that will transform the uniform waveguide of the planar geometry into a channel waveguide of cylindrical geometry. Such a transitional structure could then be used to match the cylindrical geometry of

the fiber to the planar geometry of the uniform waveguide, replacing the fiber horn.

## 2. PROGRESS IN RESEARCH

The original idea of fiber-film coupling using the step index transitional waveguide was illustrated in Fig. 4 of the proposal.[1] Ideally, it consists of step etching a GaAs waveguide as shown in Fig. 1a, followed by the deposition of a low index buffer layer as shown in Fig. 1b, and finally the deposition of a low index waveguiding layer as shown in Fig. 1c. The index of the buffer layer and the waveguiding layer should be low enough so that the propagation wave number $\beta$ in the tapered region will decrease from a value slightly above the $\beta_s$ value of the fiber at the beginning of the taper to a value lower than the $\beta_s$ value of the fiber at the end of the taper. When this tapered waveguide section is placed adjacent to a fiber with cladding removed as shown in Fig. 1d, the energy in the transitional waveguide will be transferred to the fiber via the evanescent fileds at the location where $\beta$ is matched to $\beta_s$. The role of the fiber horn is to make the transition from the flat fiber geometry to the round fiber geometry with little loss of energy.

The advantage of the proposed approach, as compared to an entirely adiabatic approach,[2-4] is that direct excitation is used to couple the transition waveguide to the primary waveguide avoiding the extremely large scattering loss of the adiabatic method.[5] The advantage of the proposed approach to the direct excitation method[6-11] is that the alignment of the two waveguides is accomplished by sputtering processes that have much better dimensional control than any mechanical process. The transitional

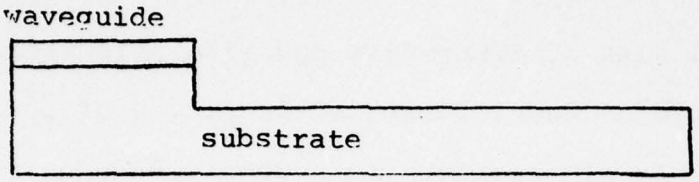


(a) the step etch

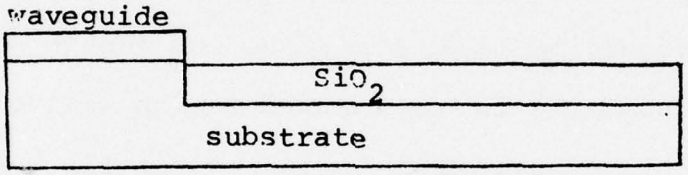


(b) deposition of the buffer layer

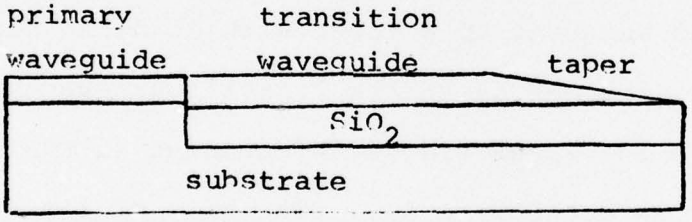


(c) deposition of the transition waveguide

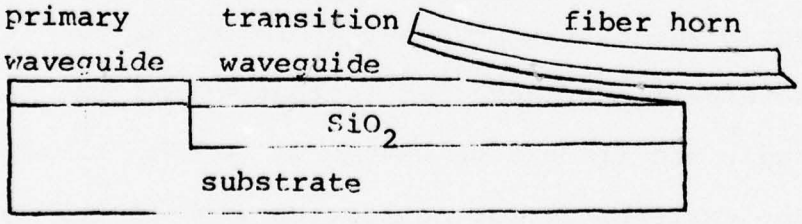


(d) coupling to the fiber

Fig. 1 Illustration of the Basic Coupling Scheme

waveguide is then coupled to the fiber by the tapered velocity coupling method which has already been shown to be efficient[2,12] and not as sensitive to mechanical misalignment as the direct excitation of fibers. The important issues to be resolved by this research contract are: (a) Can such a coupler be achieved realistically by present technology to yield high coupling efficiency. (b) If not, what are the necessary modifications.

Ideally, if all the transitions are sufficiently gentle and smooth, adiabatic transition of energy (i.e., 100 percent efficiency) will take place at all the junctions in the proposed coupling schemes, except at the step etched junction. At this junction, reflection and radiation loss will occur. In addition, there will be some energy leakage from the low index waveguiding film to the GaAs substrate because of the finite thickness of the buffer layer. A total theoretical efficiency of 80 percent was expected when we originally proposed the scheme. Since the contract began, the following calculations have been undertaken to assess theoretically the significance of various experimental conditions.

(a) Calculation of the reflection and radiation losses at the step etched junction.

(b) Calculation of the attenuation of the guided wave mode as a function of the buffer layer thickness.

(c) Calculation of the requirements of the tapered slopes to achieve adiabatic transitions to the fiber.

In practice, there will always be attenuation of guided waves in any waveguide. There will always be some energy leakage from the transitional waveguide to the GaAs substrate via the buffer

layer (called mode sinking in integrated optics). Any defects at the step etched junction caused by the fabrication process (whether these defects are random scatter centers or imperfact junction profiles) will create radiation loss or decollimation of the guided wave beam. Any mismatch of the field distributions of the waveguide modes at two sides of the junction will cause additional reflection and scattering losses. The tapered velocity coupling of the fiber and the transitional waveguide will have less than 100 percent efficiency if the taper slope is not sufficiently gentle, if the coupling of the evanescent field is not sufficiently strong, or if the surfaces are too rough. The fiber horn will have excessive mode conversion loss if the transition is not gentle enough and if the cladding surface has many defects. In short, our experimental research program is to fabricate and evaluate these structures and to obtain a realistic assessment of the performance characteristics that can be achieved by means of the present technology.

In this initial period of research, we have concentrated our effort in theoretical calculations and experimental evaluation of (a) the fabrication and the evaluation of the coupling efficiency of the step etched junction and (b) the search for a transitional structure that will match the cylindrical geometry of the fiber to the planar geometry of the uniform thin-film waveguide (e.g., the fiber horn). We think these are the two most pressing issues which must be investigated in order for the proposed coupling scheme to succeed.

## 2.1 The Step Index Transition Waveguide

There are four crucial steps in the fabrication of a step index transitional waveguide: (a) a nearly vertical and smooth surface must be obtained in GaAs waveguide by etching. (b) A sufficiently thick buffer layer must be deposited free of defects. (c) The deposited waveguide film must join the GaAs waveguiding layer in such a manner that will allow efficient transfer of energy. (d) Finally, appropriate materials (i.e., materials with appropriate index of refraction) must be used for the waveguiding film and the buffer film to enable efficient coupling to the fiber by the taper velocity method.

### 2.1.1 The Step Etch

It is well known that sputter etching or ion milling can provide very good horizontal resolution, normally limited by the definition of the mask. The vertical profile and the maximum depth of the etching are determined, to a large extent, by the thickness and the material properties of the mask.

We have experimented with conventional photolithogrpahy masks and found them to be unsatisfactory. However, when we used a cleaved piece of GaAs as a mask, we obtained excellent results. Such a mask gives us both a good horizontal edge and large vertical etching depth. Figure 2 shows a Dektak trace of the profile of the step etch in a GaAs/GaAsP waveguide (Sample No. 6-241). It shows that excellent horizontal surface condition and accurate thickness control can be obtained in this process. The slight ripple shown in the figure is caused by the striations of the GaAs/GaAsP waveguide. The vertical depth of this etched sample

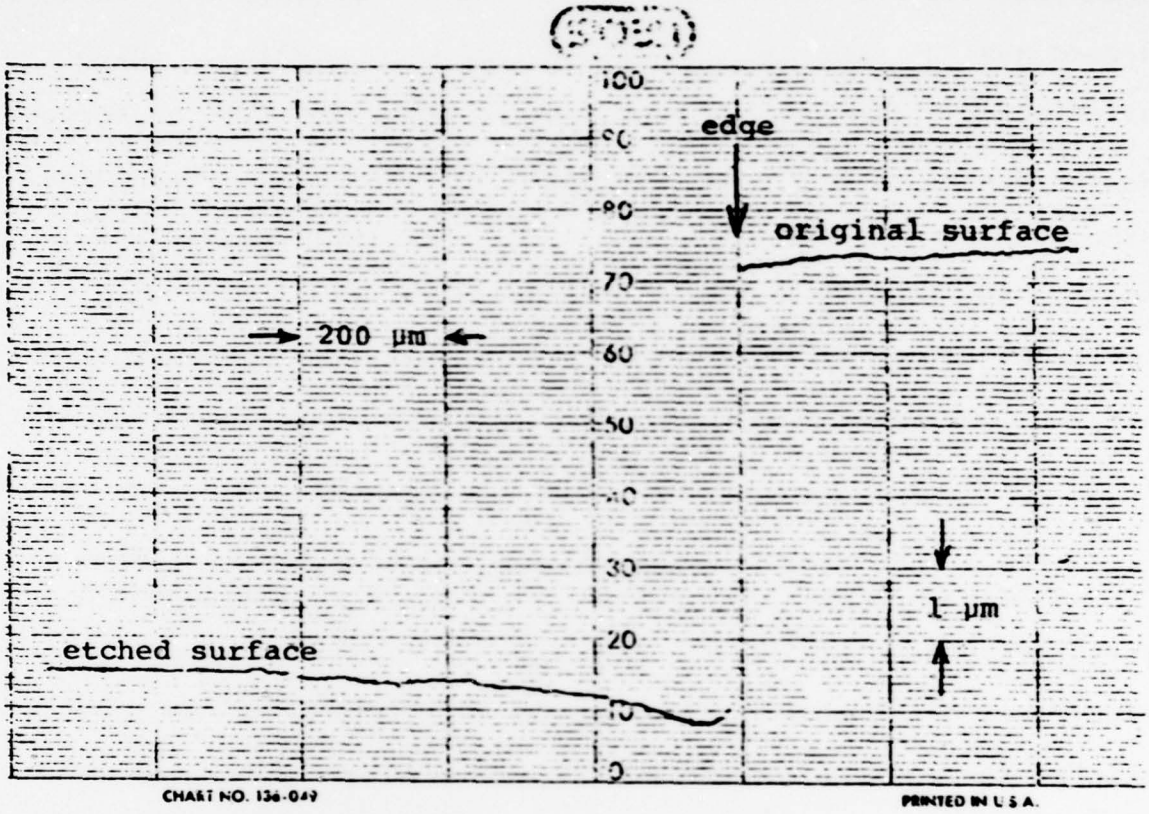


Fig. 2 Dektak Trace of the Surface Profile Near the Etched Edge

is 5.5 μm. However, because the stylus of the Dektak has a diameter of 25 μm, the resolution of the Dektak trace is too poor to evaluate the profile of the vertical edge. Figure 3 shows an optical microscopic picture of the etched edge when an $n^+$GaAs sample is cleaved in the longitudinal direction after etching. Note the excellent profile, except that the top corner was broken during the cleaving process. From such photographs we have established that the profile of the vertical edge is within 2 degrees from the desired vertical profiles. The vertical profile is critical. Our calculation shows that, if the vertical profile is more than 16.7 degrees away from the perfect vertical angle, then the energy in the GaAs guided wave will be coupled to the substrate modes of the GaAs waveguide instead of transferring into the mode of the transition waveguide. Figure 4 shows the interference pattern of the step etched sample obtained by a Watson interference microscope attachment looking directly at the top of the sample. This figure exhibits the straightness of the etched edge in the micron scale. Note that the total shift of fringes is 28 lines, confirming the etching depth obtained by the Dektak measurement. The slight curvature of the fringes near the etched edge also confirmed the Dektak result that there is a slight nonuniformity in etching depth (about 0.7 μm) within a distance of 600 μm from the mask edge. Although the effect of a thick mask on etching has not been reported in the literature, we have observed distortions of the plasma shape due to the thick mask. We have also been able to correlate the measured nonuniformity in etching thickness with the thickness of the mask.

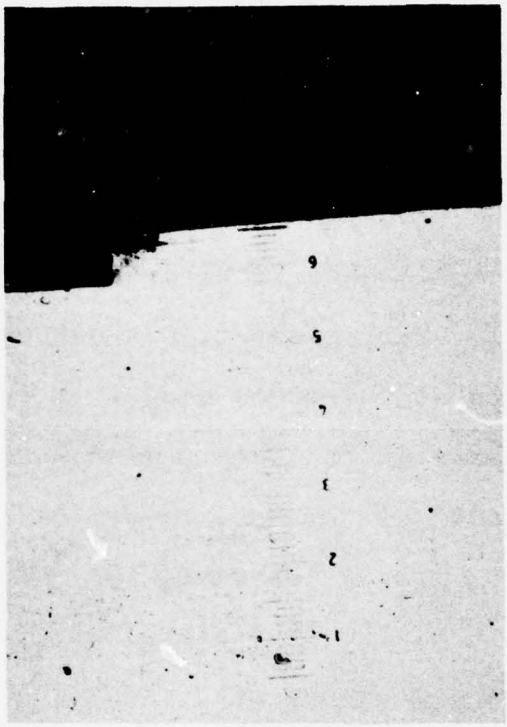

Fig. 3 Photograph of Vertical Profile of the Etched Edge on a Cleaved Surface. Vertical scale is 1.45 μm for each small division.

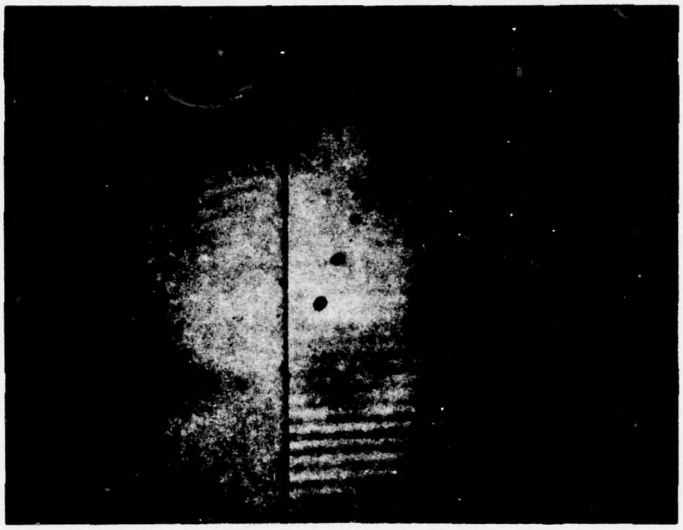


Fig. 4 Photograph of the Interference Patterns of the Etched and the Unetched Surfaces

Therefore, we believe that the nonuniformity of the electric field produced by the nonuniform plasma is the cause of the observed etching profile. Fortunately, such nonuniformity is not a great disadvantage in the fabrication of the coupler because this is a very slow variation, also its effects can be compensated in part by the subsequent deposition of the transitional waveguide.

The best way to evaluate the step etched edge is probably by measuring the radiation pattern of the edge when a guided wave in the GaAs waveguide is incident on the edge. Figure 5 shows such a radiation pattern obtained when the GaAs/GaAsP waveguide is excited by a GaAs prism coupler and an Nd/YAG laser. The radiation pattern agrees well with theoretical expectations and is well collimated in the far field, indicating that the etched edge is sufficiently smooth to not cause a substantial amount of random scattering.

The only remaining problem of the etching process that still needs to be investigated in the future seems to be related to the striation pattern of the surface roughness of the GaAs/GaAsP waveguide.[13] The striation pattern has prevented the mask from achieving continuous contact with top surface of the waveguide. Consequently, the etched edges have both the good sections and the bad sections. The typical length of the good section is on the order of 100 μm. This means that the coupler fabricated will be good only in selected sections. Since this is a problem peculiar to the GaAs/GaAsP waveguide and since such problems were not observed in the $n^+$GaAs test samples, it was decided that the investigation of this specific problem will be deferred to a later

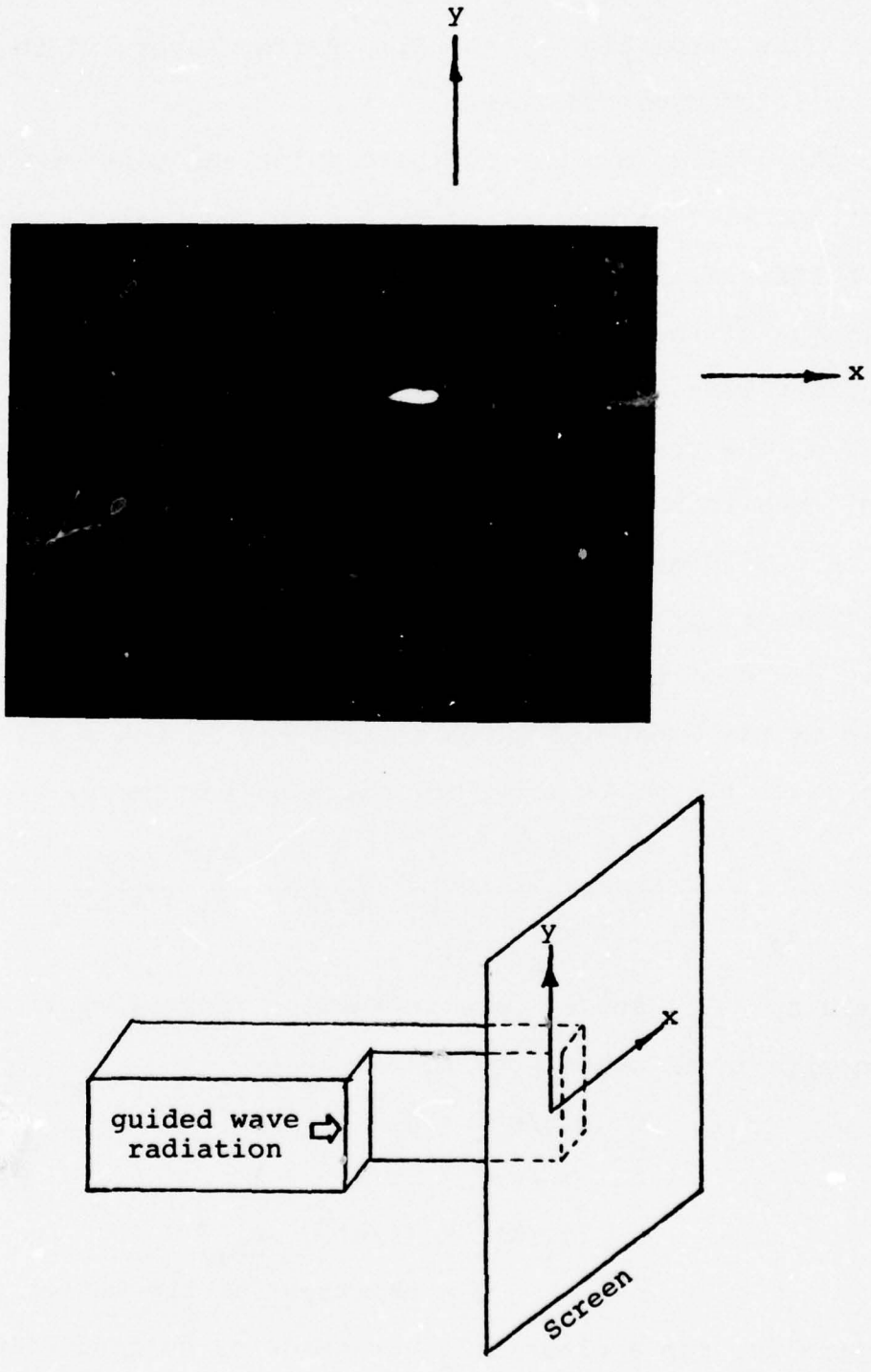


Fig. 5 A Photographed Radiation Pattern from the Step-Etched Edge

time. In the meantime, we will continue to fabricate couplers using only the good sections of the etched edge.

2.1.2 The Deposition of the $SiO_2$ Buffer Layer and the High Index Waveguide Layer

The desired minimum depth to which the GaAs waveguide should be etched will be determined by the thicknesses of the waveguiding and buffer layers which we wish to deposit. The minimum desired thickness of the buffer layer can be determined by calculating the power leaked to the high index GaAs substrate via the evanescent field of the transitional waveguide. Two approaches have been used: one is a perturbation approach where we assume that the presence of high index substrate does not change the propagation constant ($\beta$) of the low index waveguide; the other way is to solve for $\beta$ of the multilayer waveguide and then determine the field in the substrate which contributes to the power loss. In both cases the power loss, for thick buffer layers, is given by

$$P = \frac{4k\sqrt{(n_{s_2}^2 - (\beta/k)^2}}{(n_{s_2}^2 - n_{s_1}^2)(n_f^2 - n_{s_1}^2)} \quad \frac{(h/k)^2 (q_1/k)^2}{(\beta/k)\ \frac{1}{2}\ [k/p + k/q_1 + kt]}\ e^{-2q_1 d}$$

where $n_f$, $n_{s_1}$, and $n_{s_2}$ are refractive indices of film, buffer layer and high index substrate, respectively.

$$(h/k)^2 = n_f^2 - (\beta/k)^2$$

$$(p/k)^2 = (\beta/k)^2 - 1$$

$$(q_1/k)^2 = (\beta/k)^2 - n_{s_1}^2$$

$$d = \text{thickness of the buffer layer}$$

Typically, for a glass/$SiO_2$ waveguide of guiding film thickness $t = 1.5\ \mu m$, $n_f = 1.6$, $n_{SiO_2} = 1.45$, and $\beta/k = 1.58$.

The calculated attentuation rate for this waveguide due to the "mode sinking effect" is shown in Fig. 6. From this figure we may conclude that a buffer film of 2 μm thickness will be sufficient to isolate the waveguide mode from the GaAs substrate. It must be pointed out, however, that any waveguide capable of coupling to optical fiber will have an effective refractive index, $\beta/k$, close to 1.45. In that case, we need more than 5μm buffer thickness in order to obtain adequate isolation.

The desired thickness of the waveguiding layer can be determined analytically by maximizing the overlap integral between the GaAs waveguide mode and the transitional waveguide mode. Maximization of the overlap integral will ensure that the coupling coefficient between the two waveguide modes is optimized. For the normalized TE modes, the coupling efficient between mode i of GaAs and mode j of the transitional waveguide is given by

$$C_{tij} = \frac{2\beta_{1i}\,\beta_{2j}}{\beta_{1i}+\beta_{2j}} \frac{A_{1i}\,A_{2j}}{2\omega\mu} \left\{ e^{-q_{1i}a} \sin\phi_{1i} \sin\phi_{2j} \right.$$

$$+ \frac{\sin\phi_{1i}(q_{1i}-h_{2j})[\cos(h_{2j}a+\phi_{2j}) - e^{-q_{1i}a}\cos\phi_2]}{(h_{2j}^2 + q_{1i}^2)}$$

$$+ \frac{\sin[(h_{1i}-h_{2j})t_1 - ah_{2j} + \phi_{1i} - \phi_{2i}] - \sin(\phi_1 - \phi_2 - ah_{2j})}{2(h_{1i} - h_{2j})}$$

$$\left. + \frac{\sin(ah_{2j}+\phi_{1i}+\phi_{2j}) - \sin[(h_{1i}+h_{2j})t_1 + ah_{2j} + \phi_{1i} + \phi_{2j}]}{2(h_{1i} + h_{2j})} \right\}$$

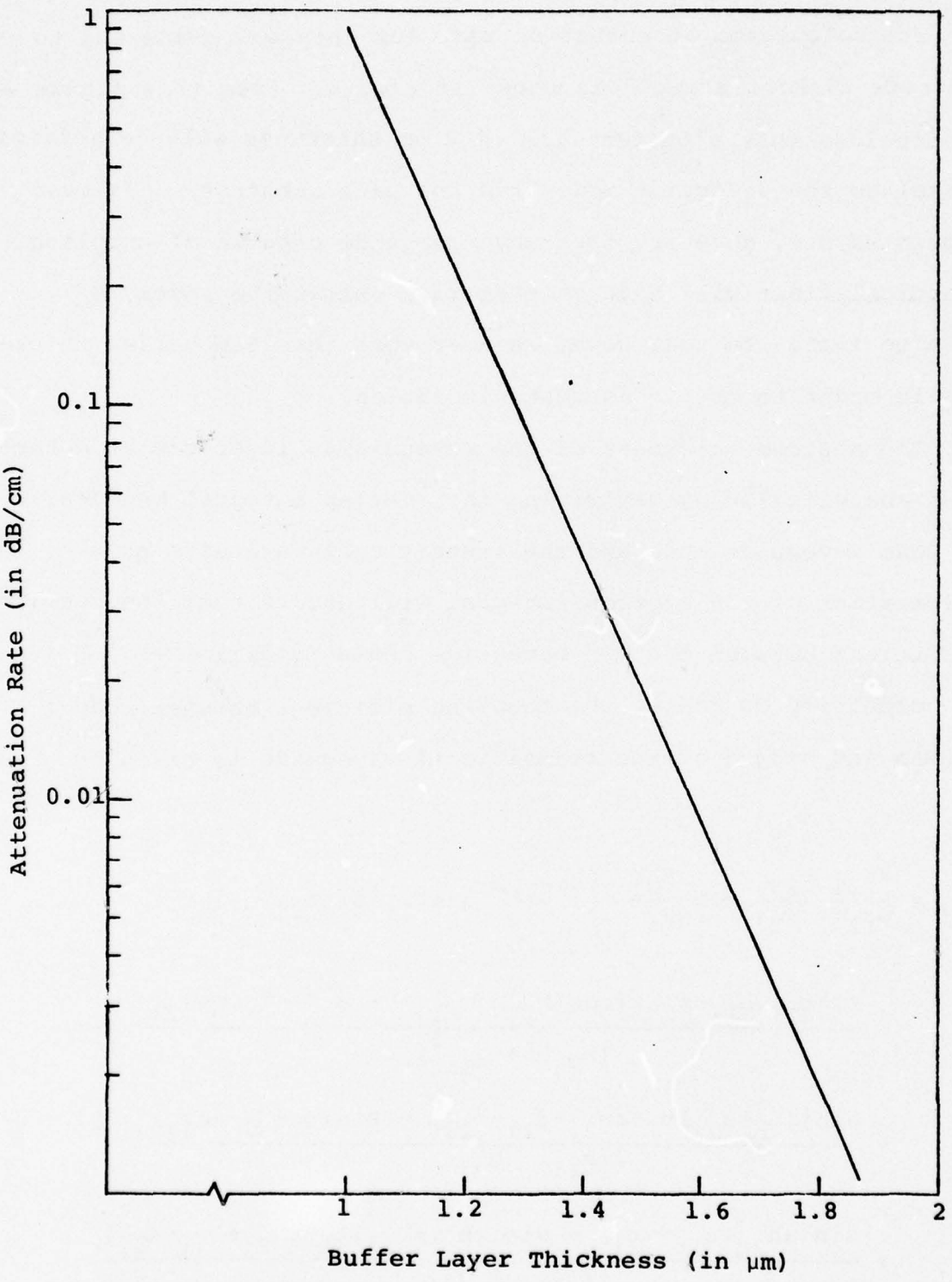


Fig. 6 Calculated Attenuation Rate of the Glass/$SiO_2$ Transitional Waveguide on GaAs

$$+ \sin(h_{1i}t_1+\phi_{1i})\left[\cos\{h_{2j}(t_1+a)+\phi_{2j}\} - e^{-p_{1i}b}\cos(h_{2j}t_2+\phi_{2j})\right]$$

$$+ \frac{e^{-p_{1i}b}}{p_{1i}+p_{2j}}\sin(h_{1i}t_1+\phi_1\ \sin(h_{2j}t_2+\phi_{2j})\Bigg\}$$

where a and b are shown in Fig. 7

$$h_{1i} = \left[n_{f_1}^2 k^2 - \beta_{1i}^2\right]^{\frac{1}{2}}$$

$$q_{1i} = \left[\beta_{1i}^2 - n_{s_1}^2 k^2\right]^{\frac{1}{2}}$$

$$\phi_{1i} = \tan^{-1}\frac{h_{1i}}{q_{1i}}$$

$$A_{1i}^2 = \frac{2\omega\mu_0}{\beta_{1i}}\frac{1}{\left[\frac{t_2}{2}+\frac{1}{2p_{1i}}+\frac{1}{2q_{1i}}\right]}$$

and similar expressions for $h_{2j}$, $q_{2j}$, $\phi_{2j}$, and $A_{2j}$. Subscripts 1 and 2 refer to GaAs and transition waveguides, respectively. $n_f$ and $n_s$ are the refractive indices of film and substrate, and t is the film thickness.

In practical situation $TE_0$ mode is of most interest due to its lowest loss; in this case it is important to know how $TE_0$ mode of waveguide 1 is coupled to other modes of waveguide 2. Assuming the guiding layers are thick, i.e., $\beta_{1j}\simeq n_{f_1}k$ and $\beta_{2j}\simeq n_{f_2}k$, the power coupling coefficient $|C_{tom}|^2$ can be written as

$$|C_{tom}|^2 = \frac{64}{\pi^2}\frac{n_{f_1}n_{f_2}}{\left(n_{f_1}+n_{f_2}\right)^2}\frac{t_1}{t_2}\frac{1}{\left\{1-\left[(m+1)\frac{t_1}{t_2}\right]^2\right\}^2}\cos^2\left[\frac{(m+1)\pi t_1}{t_2}\right]\sin^2\left[\frac{(m+1)\pi}{2}\right]$$

Figure 7 shows $|C_{tom}|^2$ as a function of $\frac{t_2}{t_1}$ for $GaAs_{0.77}P_{0.23}$/ $GaAs_{0.66}P_{0.34}$ waveguide to AZ 1350/$SiO_2$ waveguide.

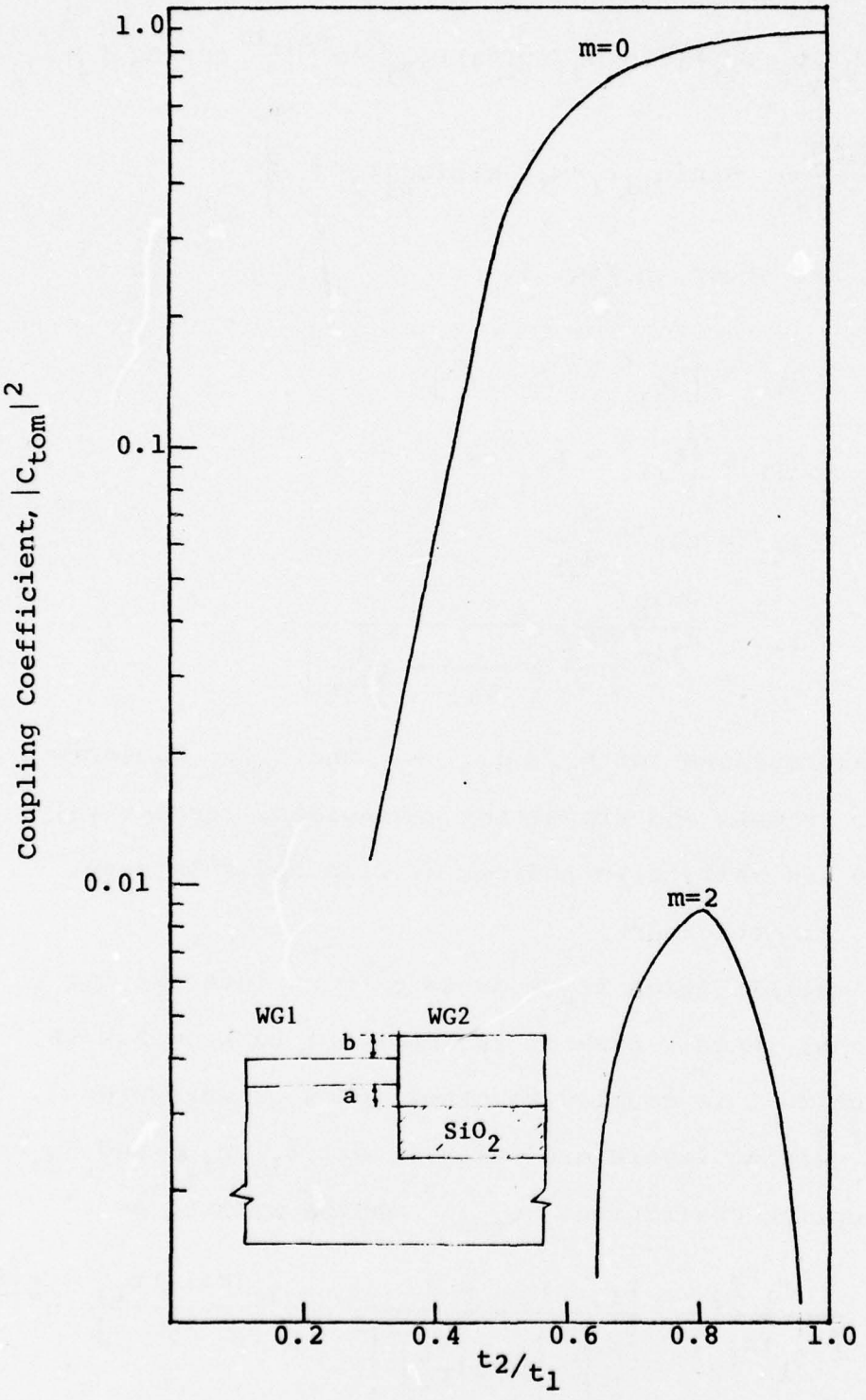


Fig. 7 Calculated Coupling Coefficients Between the GaAs and the Transitional Waveguide

Typically, our GaAs/GaAsP waveguides have a film thickness of 1.5 μm. Based upon the preceding analysis, we determined that the desired etching depth is 7 μm, the desired buffer thickness of $SiO_2$ films is 6 μm, and the desired waveguiding film thickness is 1.5 μm. In GaAs/GaAsP waveguide, sample No. 6-242, we etched a step 7.5 μm deep and then deposited an $SiO_2$ layer in the etched section 6 μm thick according to the above plan. The etching and the deposition were done in one process witnout moving the sample or the mask in the bell jar. Figure 8 shows the radiation pattern of the step with the $SiO_2$ layer. Notice the various expected lobes of the radiation pattern. Notice also that there are two beams in the main lobe. This indicates that the radiation is coming from two sections illuminated by a single guided wave beam. It illustrates the difficulty with GaAs/GaAsP waveguide discussed in Section 2.1.1. Moreover, when we cleaved a test sample which had been placed next to the waveguide sample in the same run, we discovered under the optical microscope that there are $SiO_2$ deposits on the vertical wall of the edge. Clearly, the vertical layer of $SiO_2$ will cause a degradation of the coupling coefficient between the two waveguide modes. How to remove (or how to prevent) the deposits of $SiO_2$ on the vertical surface is a research area where further investigation will be conducted in the next period. In the meantime, we decided to investigate the performance of this imperfect step junction (including the vertical $SiO_2$ layer).

For this purpose we coated a layer of AZ 1350 photoresist on top of the $SiO_2$ layer, approximately 2 μm thick. AZ 1350 photo resist was used because it is transparent at 1.06 μm. Since AZ 1350

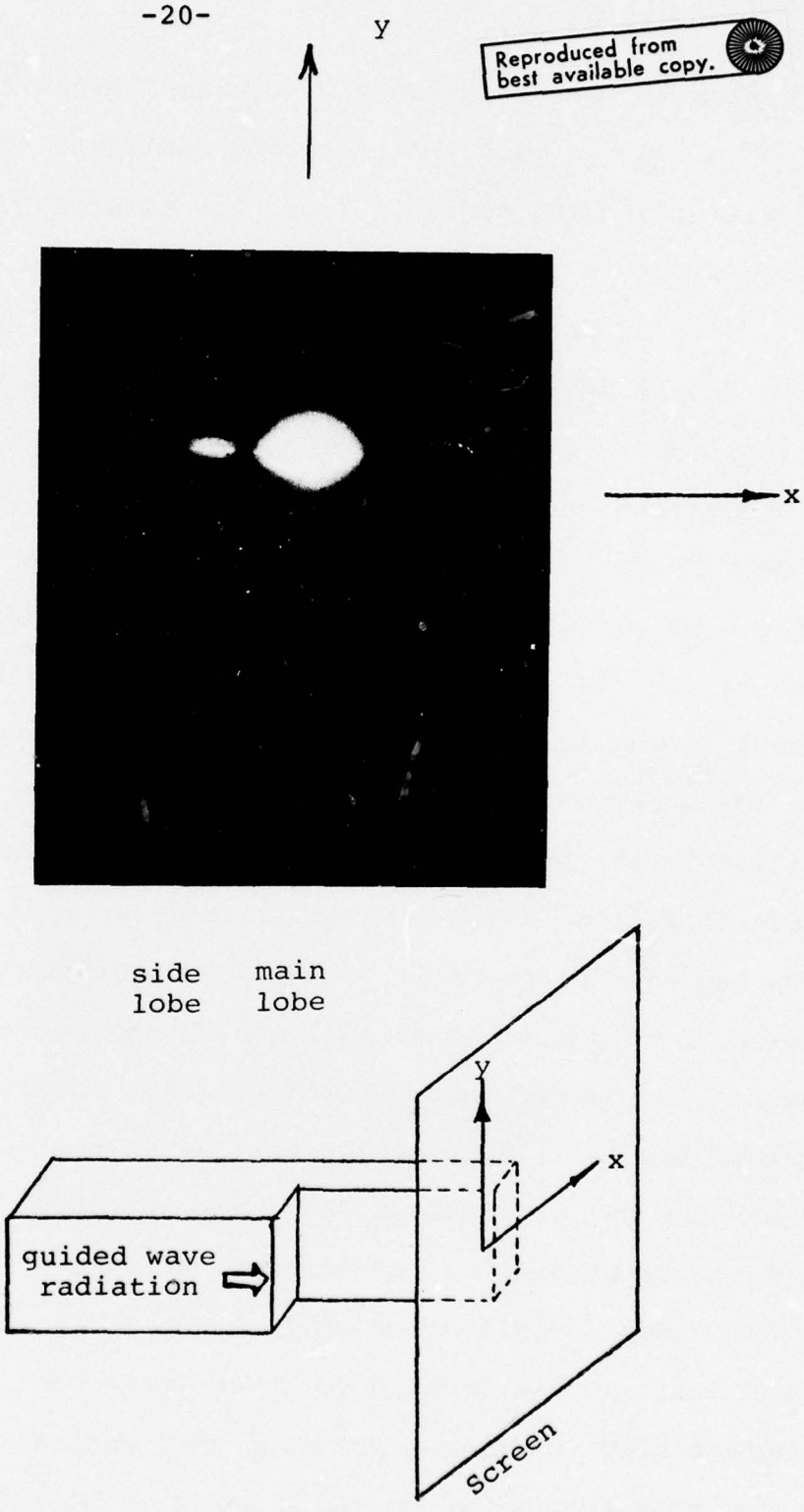


Fig. 8 The Radiation Pattern of the GaAs Waveguide Step-Etched Edge

is a liquid, it also fills up any nonuniform region of the $SiO_2$ layer near the junction. In order to evaluate this transitional waveguide a guided wave m = 0 mode was excited by a GaAs prism coupler on the GaAs waveguide side. This GaAs/GaAsP waveguide has only one propagating TE mode, $TE_0$. Figure 9 shows that the optical radiation continued past the junction as the guided mode of AZ 1350/$SiO_2$, without any noticeable scattering at the junction. Using a rutile prism as the output coupler, we found that the power in the transitional waveguide was predominantly in the $TE_0$ mode. We have also evaluated this junction in the reverse direction. When the AZ 1350 waveguide was excited for the m = 0 mode, its power was also coupled into the $TE_0$ mode of the GaAs waveguide. When the m = 1 mode was excited on the transitional waveguide, no power was coupled into the $TE_0$ mode of the GaAs waveguide. This clearly indicates that highly preferential coupling between same order modes was obtained in such a junction, confirming qualitatively the calculated results obtained for the coupling coefficient.

The power coupled from the GaAs into the AZ 1350 waveguide was determined by measuring the guided mode power in the AZ 1350 waveguide at various distances from the step. By extrapolation, we obtained the power coupled into the AZ 1350 guide just at the junction. The power transmitted by the prism and the GaAs waveguide to the junction is determined by evaluating the attenuation rate and the input prism coupling efficiency of a second waveguide, cleaved from the same GaAs/GaAsP wafer as the test waveguide. From this measured data and the data of the laser power,

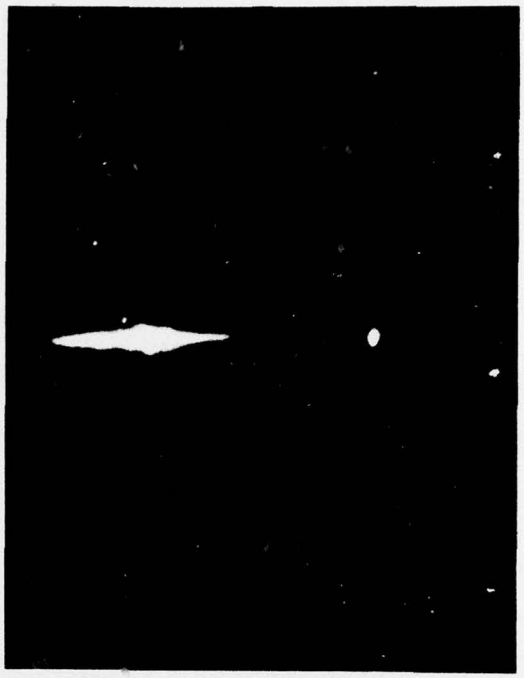


Fig. 9 Photograph of the Scattered Radiation from the GaAs Waveguide and the Transition Waveguide

we calculated the power incident to the step junction. The ratio of the two powers is the coupling efficiency. A measured coupling efficiency of 77 percent was found by this method.

Naturally, we are much encouraged by the measured high efficiency. But the AZ 1350 waveguide is physically too soft to be a useful permanent waveguide. Therefore, we have begun to investigate sputtering a $BaO_2$-$SiO_2$ waveguide to be used as the transitional waveguide.

2.1.3 The Hollow Dielectric Transitional Waveguide

Note that sputtered $SiO_2$ was used for the buffer layer in the experiments discussed in Section 2.1.2 because its sputtering properties have been thoroughly characterized. Unfortunately, sputtered $SiO_2$ will give a $\beta$ value of the tapered waveguide higher than the $\beta$ values of the fiber. In order to meet the requirements of the $\beta$ values for phase matching, we can either use materials such as $CaF_2$ or $MgF_2$ for the buffer layer, or use the hollow dielectric mode in the waveguide. We have investigated in this period the hollow dielectric mode as the transitional waveguide.

In short, the hollow dielectric mode can be represented as plane waves bouncing between two dielectric interfaces, as shown in Fig. 10. In the conventional waveguide the reflection at the interface with the substrate is a total internal reflection. In this case, the index of the substrate is considerably higher than the index of the film. Thus the reflection at that interface has a transmitted beam as well as a reflected beam. Since the index of GaAs is much higher than the index of $SiO_2$ and since the plane waves are incident at the interface with an almost

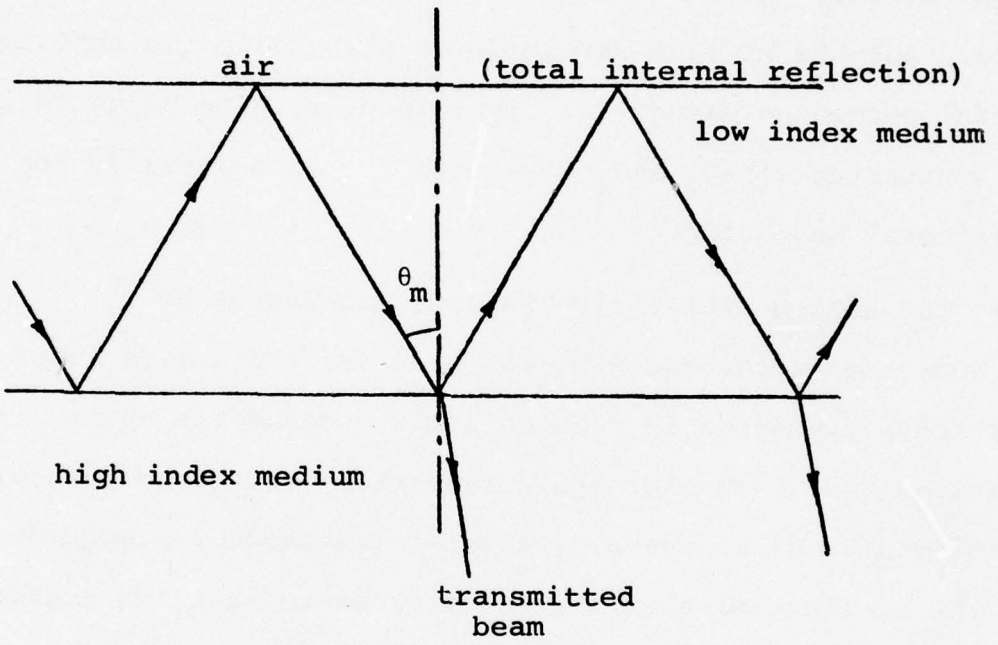


Fig. 10 Plane Wave Representation of the Hollow Dielectric Waveguide

grazing angle, the energy loss to the transmitted beam is small. Thus the hollow dielectric mode is similar to the conventional waveguide mode, except that it is a leaky mode. Such a hollow dielectric mode was used in waveguide gas lasers.[14-16]

Our interests in the hollow dielectric waveguide mode are: (a) its low attenuation. (b) Its $\beta$ values are typically just below the value of $n_b k$, matching approximately the $\beta$ values of the fibers. Her $n_b$ is the index of the buffer film and k is the free space propagation wave number.

During this contract period, we have first calculated the propagation wave number of $\beta_h$ of such a hollow dielectric waveguide. The equation for the $\beta_h$ can be obtained similarly to the conventional waveguide by requiring that the round-trip phase shift of a plane wave reflected by the two dielectric interfaces be multiples of $2\pi$ radius. The equation obtained in this manner for $\beta_h$ for large film thickness is approximately

$$n_b kt \cos\theta_m - \tan^{-1}\left[\frac{\sqrt{\sin^2\theta_m - 1/n_b}}{\cos\theta_m}\right] = (2m+1)\pi/2$$

where $\theta_m$ is the angle of incidence of the plane wave representation of the mth propagating hollow dielectric waveguide mode shown in Fig. 10 (i.e., $\beta_{hm} = n_b k \sin\theta_m$); t is the thickness of the film; $k = 2\pi/\lambda$. It is clear from this equation that $\beta_{hm}$ will change as the film thickness is varied. Figure 11 illustrates such changes in $\beta_{ho}/k$ for a hollow dielectric waveguide mode in $SiO_2$ on top of GaAs. These changes demonstrate that phase matching can be achieved easily between the fiber and the waveguide by a tapered section. We have also experimentally fabricated

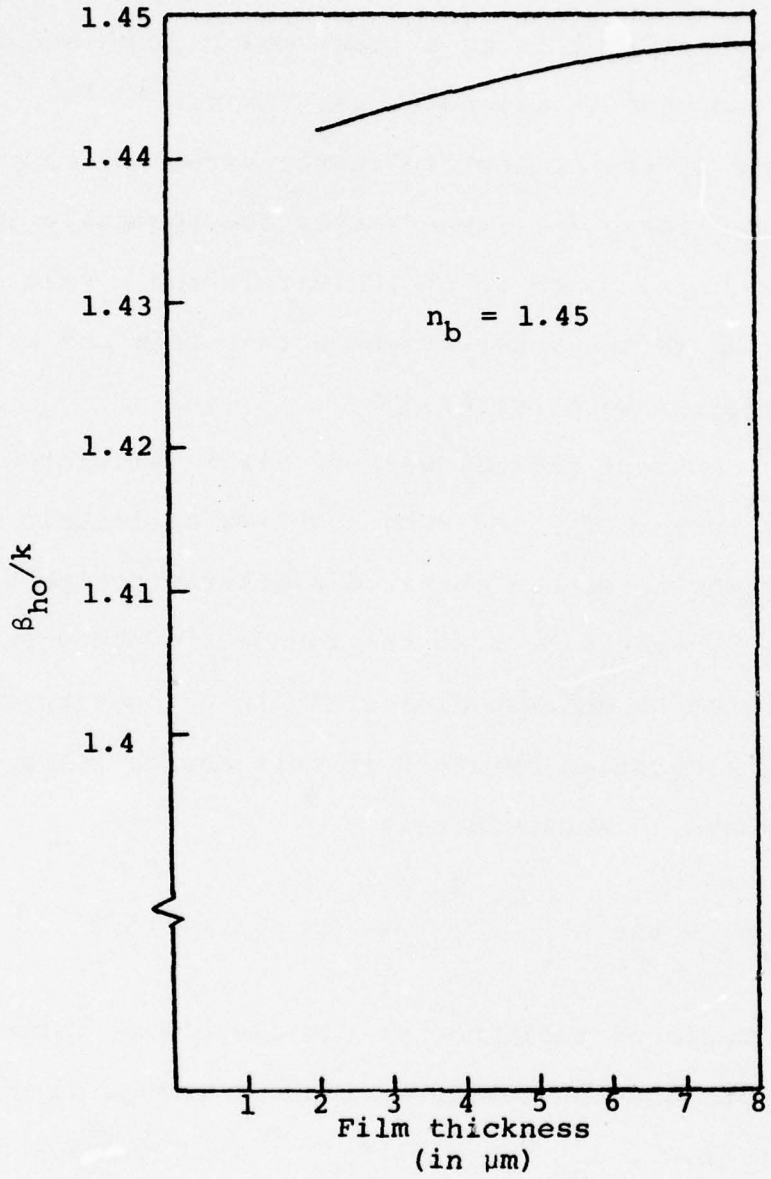


Fig. 11 Variations of the Propagation Wave Number of the Hollow Dielectric Waveguide Mode as a Function of Waveguide Thickness

hollow dielectric waveguides with $SiO_2$ layer (about 6 μm) and AZ 1350 layer (about 3 μm) on flat GaAs samples. We were able to excite these modes by prism coupler just like the usual waveguide modes. The measured values of $\beta_{hm}$ also correspond well with the calculated results.

Our next project is to calculate the attenuation rate (i.e., the leakage rate) of the hollow dielectric mode on top of the GaAs. We expect that the attenuation rate of the hollow dielectric mode would be too high to be useful for very thin films because the reflection loss at the GaAs boundary will increase very rapidly as the angle $\theta_m$ shifts away further from $\pi/2$. This is partially confirmed by the initial measured attenuation rate of the two experimental hollow dielectric waveguides.

The necessity of using a large waveguide thickness for the hollow dielectric waveguide mode may be an important disadvantage of this type of transitional waveguide, because the overlap integral may be quite small between the guided wave mode of the GaAs epitaxial waveguide and the hollow dielectric mode desired for coupling to the single-mode fibers. We expect that a theoretical analysis will be carried out during the coming contract period to answer this question.

## 2.2 The Fiber Horn

The initial idea was to heat an existing fiber to its plastic temperature range and then to apply mechanical pressure to the softened fiber to deform it into an elliptical shape. If such a horn can be fabricated without creating excessive

scattering loss, the dominant mode of the fiber core will be transformed adiabatically into the dominant mode of the elliptical fiber. The mode of the elliptical fiber will have a long evanescent tail because the thickness of the core is small. Additionally, the cladding material will be thin. Consequently, there will be a significant amount of the energy in the evanescent tail outside of the cladding material in the air, convenient for the coupling to the waveguide by the tapered velocity coupling method. The broadened width of the elliptical waveguide means also that the beam, once coupled into the waveguide, will remain collimated in the horizontal direction. The key to success is naturally how to deform the fiber without creating a large number of scattering centers.

During this contract period, we have investigated experimentally the fabrication of such a fiber horn by two different methods. These experiments are discussed in the following sub-sections. From these experimental results, we concluded that the difference of the thermal properties of the cladding and core material will not allow us to fabricate a low-loss fiber horn in silica-borosilicate fibers by this method.

2.2.1 The Fabrication of the Fiber Horn by $CO_2$ Laser Direct Heating

Initial experiments were conducted with multimode glass fibers in order to evaluate and to optimi e the basic mechanical process involved in heating a cylindrical fiber and forming it into the desired taper. $CO_2$ laser radiation was used to heat the fiber because it is clean, its power can be controlled

accurately, and it is absorbed effectively by the fiber. A variable pressure pneumatic press was used to force a replaceable form vertically down against another such form. The surfaces of the two forms were optically polished to a planar configuration, and the relative angle and position of the lower form was acurrately adjustable by micrometers. By preheating the last few millimeters of the glass fiber using side illumination from the $CO_2$ laser, a tapering section of up to 2 mm in length was produced by the controlled, rapid pressing of the plasticized fiber between aluminum forms.

This initial success with the glass fibers encouraged us to fabricate next the horns with multimode silica fibers. Anticipating the high softening temperature of the silica fiber, optically polished molybdenum was used for the mechanical forms. Molybdenum was chosen because of its high reflectivity at 10.6 μm, its high melting temperature, and its suitability for maintaining optical flatness under pressure. In order to obtain sufficient energy density, the 50-watt, 10.6-μm CW laser radiation was focused onto the end of the fiber. However, the absorption coefficient of silica at 10.6 μm wavelength is so high and the thermal conductivity of the silica sufficiently low that the end of the fiber evaporated before a useful length (less than 1 mm) was heated above the softening temperature. Pulsing the laser radiation would give us much more accurate control of the heating of the fiber. We have pulsed the $CO_2$ laser and varied both the width and the repetition rate of the pulse at different power levels so that the maximum volume of the fiber was heated up to a temperature

below evaporation. Evaporation was prevented by this method; but the pliable length of the fiber remained very small.

In order to provide the necessary thermal environment, high density polished graphite forms were substituted for the Molybdenum forms and $CO_2$ laser radiation was used to heat the forms, achieving an oven-like effect. However, 50 watts of $CO_2$ laser radiation was insufficient to heat up both the fiber and the graphite forms to a sufficiently high temperature. Subsequently, electrical resistive heating of the graphite form was used to soften the silica fibers.

2.2.2 The Fabrication of the Fiber Horn by Electrical Resistive Heating

In this second method, the lower polished graphite form served also as the resistance heater. The upper form was appropriately remounted to provide the necessary tapering adjustment. A nitrogen atmosphere at 10 psi pressure was maintained around the pneumatic jig to prevent the oxidation of graphite. The forming process was observed by means of a stereo microscope positioned between the two forms at the tapering end of the fiber. The temperature of the fiber was monitored by an optical pyrometer.

Experimental results indicate that a sufficient amount of uniform heating can be produced by this method without oxidation of the graphite. Tapers with angles as small as 4° can be produced over a length of 1.5 mm. However, the softening temperature of the borosilicate cladding of the fibers was measured to be approximately 1325°C. At the softening temperature of the $SiO_2$ core, approximately 1625°C, the borosilicate cladding appears to liquefy

and tends to attach to the graphite form. A number of horns from both the multimode and the single-mode fibers have been produced in this manner with the fibers heated to not more than 1650°C. In an attempt to minimize unnecessary heating of the borosilicate material, the temperature of the graphite form was controlled by feedback from the optical pyrometer. Best results were obtained with the lowest applied pressure to the form. Measurements of the produced horns before removal from the lower form indicate horns of the length of 2 mm and thickness of 20 μm have been obtained, corresponding to a cross-sectional aspect ratio of 15 to 1 at the end of the horn. Figure 12 is a photograph of a typical single-mode fiber horn fabricated in this manner. Notice the very poor surface quality. The center white line is the core. In this particular case, the core seems to be intact while the cladding has already been badly corrugated. Fiber horns obtained by heating to a higher temperature showed a much greater degree of surface degradation. Removal of the tapers from the lower forms always resulted in the breakage of the horn at a thickness of approximately 35μ due to the adhesion of the borosilicate glass to the form.

From these results, we reached several conclusions: (1) Obviously the silica fiber is made with core and cladding materials that have very different thermal properties. Figure 13 shows the photograph of an illuminated end of a single-mode silica fiber donated to us by Bell Telephone Laboratories. This picture illustrates the three separate layers of the fiber, the core, the cladding; and an outer sleeve consists of silica. (2) When a silica

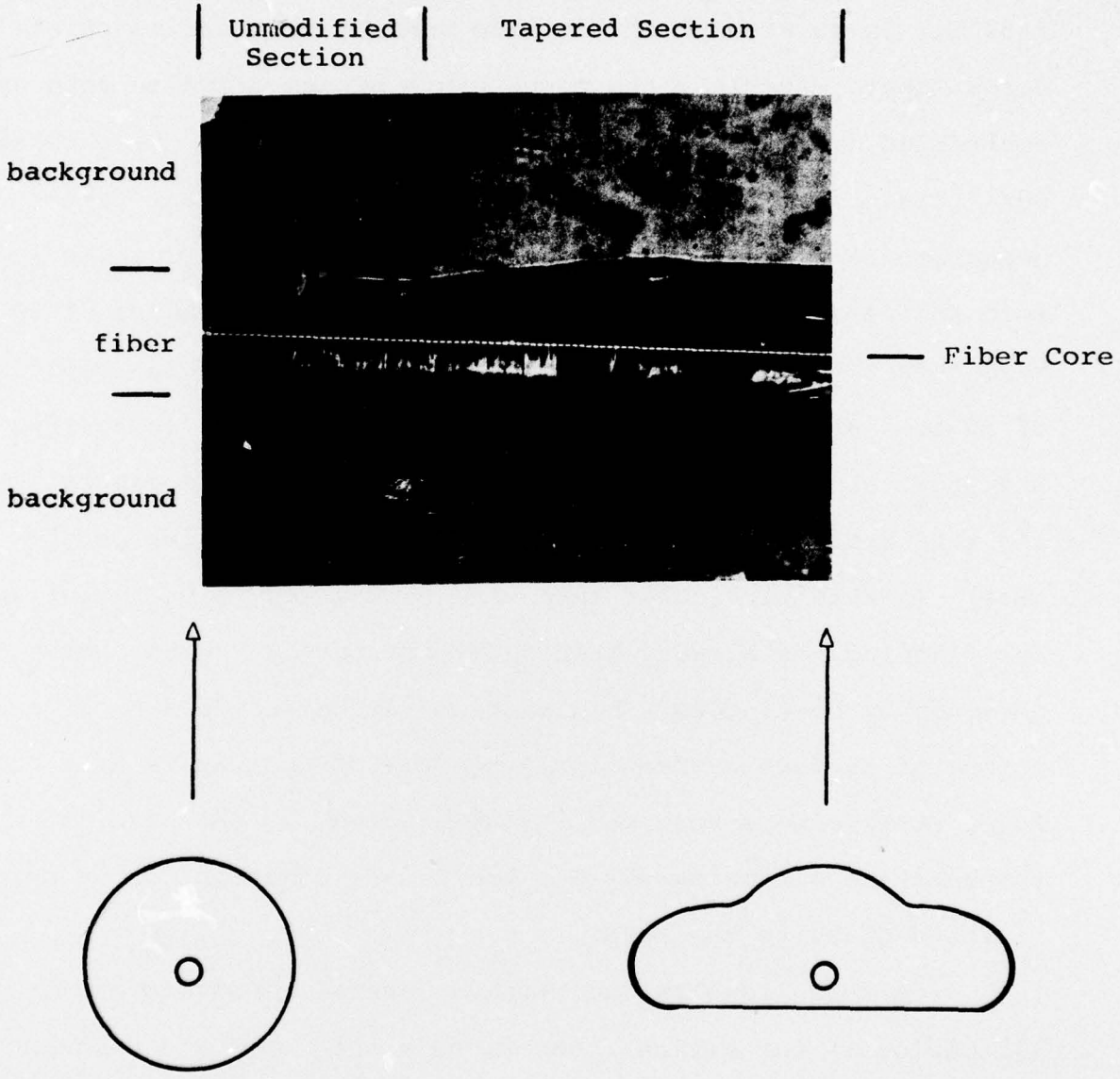


Fig. 12 Photograph of Single-Mode Fiber Horn

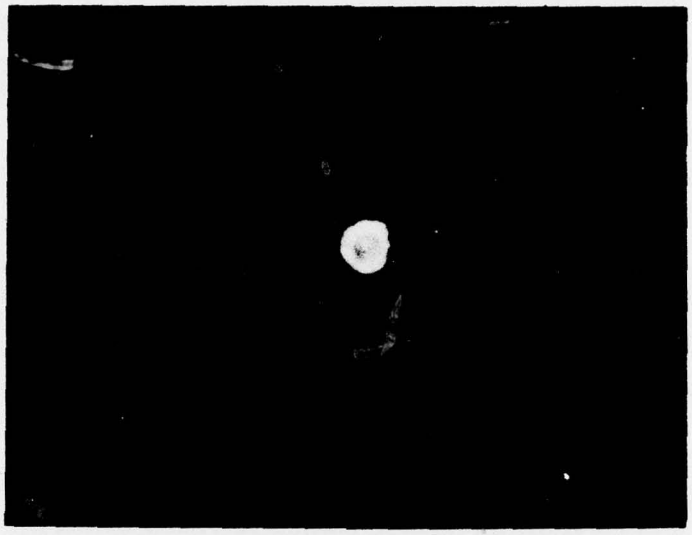

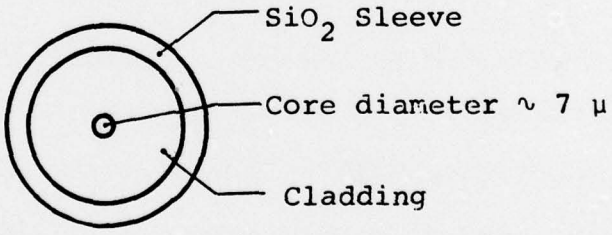


Fig. 13 Photograph of the Single-mode Fiber Cross-section

fiber is heated to a temperature between 1325°C and 1625°C, the cladding is softened enough to be deformed. But the core and the sleeve remain cylindrically solid. When mechanical pressure is brute-forcely applied to change the shape of the cladding, the surface quality becomes very poor because of the inhomegenous deformation process. (3) If the borosilicate cladding is heated to its liquid state, the adhesion of the fiber to the form is much worse, and a much poorer taper is obtained. In short, the drastically different thermal properties of the cladding and the core have prevented the silica fiber from deforming uniformly in the plastic temperature range. This is a fundamental bottleneck to the fabrication of silica fiber horns by any form of heating process. Nevertheless, the ability to deform the cladding without deforming the core may be very useful. For example, it may be used to remove cladding materials from the core in the future.

## 2.3 Transitions from the Planar Waveguide to the Cylindrical Fiber

We discussed in the previous sections the reasons why the horn cannot be fabricated with silica fibers. Alternative methods must now be found. One alternate method for fabricating a fiber horn has already been reported by Dalgoutte, et al.,[2] in that an externally mounted glass fiber horn was fabricated by drawing it from a glass pre-form. On the other hand, there is no reason that a transition from a uniform thin-film waveguide to a channel waveguide configuration cannot be made either within the GaAs waveguide or the transitional waveguide. If there is such a transition, the fiber can then be coupled by evanescent field dirrectly to a tapered channel waveguide when its cladding is sufficiently removed.

The disadvantage of Dalgoutte's method is that the externally mounted fiber still needs to be interconnected with the single-mode fused silica fiber for transmission. The disadvantage of using a channel waveguide is that the horizontal position alignment is critical between the core and the channel. However, recent trends in integrated optics research (see, for example, the technical digest of the 1976 Topical Meeting in Integrated Optics) indicate that a monolithic integrated optical subsystem may utilize channel waveguides in GaAs. In that case, since channel waveguides have already been used in GaAs, we may as well use a channel transitional waveguide for coupling into fibers.

Based upon the preceding reasons, we have initiated research in this contract to investigate propagation characteristics and insertion loss of tapering of uniform glass waveguide into channel glass waveguides. Two forms of tapering structures are being investigated. In the first form, metal patterns, such as those shown in Fig. 14a, will be produced because of the complex dielectric constant of the metal films. In the second form, shown in Fig. 14b, masked ion exchange of Ag ions with Nd ions will be used to obtain a diffused tapering structure. Glass is chosen here because we expect the transitional waveguide will be made by sputter deposition of glass on $SiO_2$. In this manner, the technology developed will be directly applied to the transitional waveguide under development as discussed in Section 2.1. The results of this investigation will be discussed in the next progress report.

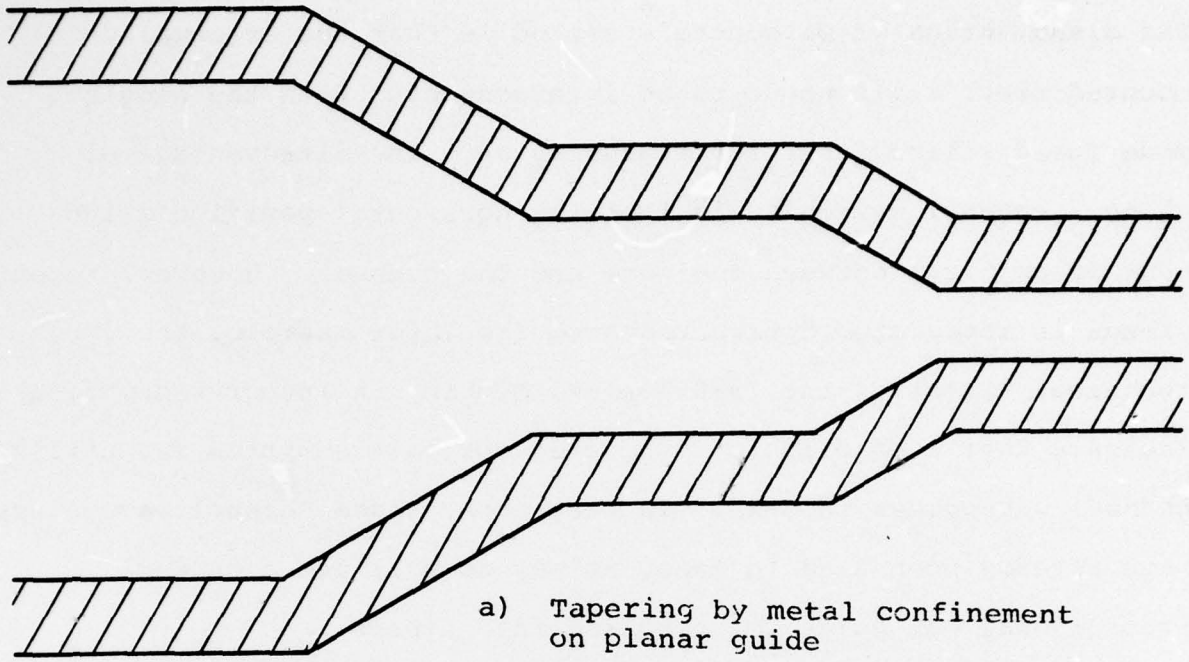

a) Tapering by metal confinement on planar guide

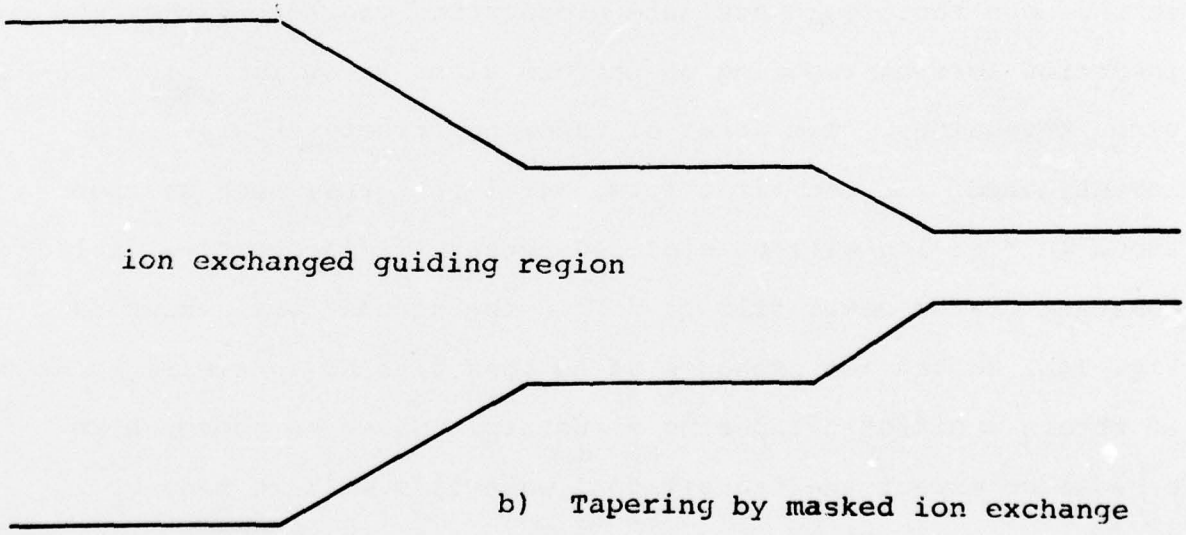


b) Tapering by masked ion exchange

Fig. 14 Taper structures for conversion of Uniform Waveguide into Channel Waveguide

## 3. WORK FOR THE NEXT PERIOD

A. Full evaluation of the step-etched transitional waveguide with sputtered glass film on $SiO_2$ buffer layer.

B. Evaluation of the excitation of hollow dielectric waveguide mode.

C. Investigation of the tapering of uniform waveguide to channel waveguide (in both glass waveguides and GaAs waveguides). Emphasis will be placed on evaluating the insertion loss and establishing the fabrication procedures.

D. Investigation of the various ways to strip the cladding from the single-mode fiber.

## 4. ARTICLES PUBLISHED

B. L. Sopori and W. S. C. Chang, "Evaluation of GaAs Heterostructure Waveguides for 1.06 μm and 0.905 μm Wavelength", Applied Optics, Vol. 15, p. 789, 1976.

REFERENCES

1. Proposal on "Efficient Coupling of Fibers to GaAs Waveguides", submitted by the Laboratory for Applied Electronic Sciences, Washington University, to Air Force Cambridge Research Laboratories, February 15, 1975.

2. D. G. Dalgoutte, R. B. Smith, G. Achutaramayya, and J. H Harris, "Externally Mounted Fibers for Integrated Optics Interconnections", Appl. Optics, 14, p. 1869, 1975.

3. W. S. C. Chang, H. P. Hsu, A. F. Milton, B. L. Sopori, and R. A. Becker, "Coupling of Single-Mode Fibers to Thin-Film Waveguide - A Progress Report", Proceedings of Electro-optical Systems Design Conference, p. 228, 1975.

4. D. G. Dalgoutte, G. L. Mitchell, R. L. K. Matsumoto, and W. D. Scott, "Transitional Waveguide for Coupling Fibers to Semiconductor Lasers", Appl. Phy. Lett., 27, p. 125, 1975.

5. H. P. Hsu and A. F. Milton, "Mode Lift-off Using a Branching Dielectric Waveguide", Paper WD8 presented in Topical Meeting of Integrated Optics, Salt Lake City, Utah (1976).

6. L. P. Boivin, "Thin Film Laser-to-Fiber Coupling", Appl. Opt., 13, p. 391 (1974).

7. D. L. Bisbree, "Optical Fiber Joining Technique", B.S.T.J., 50, p. 3153 (1971).

8. R. G. Hunsperger and A. Lee, "Parallel End-Butt Coupling of a GaAs Laser Diode and a Thin Film Waveguide", Paper WD4 presented in Topical Meeting of Integrated Optics, Salt Lake City, Utah (1976).

9. E. Weider, "Light Coupling from a Junction Laser into a Monomode Fiber with a Glass Cylindrical Lens on the Fiber End", Opt. Comm. 12, p. 93 (1974).

10. C. A. Brackett, "On the Efficiency of Coupling Light from Strip Geometry GaAs Laser into Multimode Fibers", J. Appl. Phys, 45, p. 2636 (1974).

11. J. Guttman, O. Krumphalz, and E. Pfeiffer, "Optical Fiber-Stripline-Coupler, Appl. Optics, 14, p. 1225, 1975.

12. R. A. Becker, Experimental results obtained at Washington University.

13. B. L. Sopori and W. S. C. Chang, "Propagation Characteristics of GaAsP Heterostructure Waveguides for 1.06 μm and 0.905 μm Wavelengths: An Evaluation", Appl. Optics, 15, p. 789, 1976.

14. P. W. Smith, "A Waveguide Gas Laser", Appl. Phys. Lett., 19, p. 132, 1971.

15. E. A. J. Marcatili and R. A. Schmeltzer, "Hollow Dielectric Waveguide Modes", B.S.T.J., 43, p. 1783 (1964).

16. T. J. Bridges, E. G. Buckhardt, and P. W. Smith, "$CO_2$ Waveguide Lasers", Appl. Phys. Lett. 20, p. 403 (1972).

## Report of Expenditures

The detailed list of expenditures from August 15, 1975, through February 5, 1976:

| | |
|---|---|
| Academic Salary | $6,000.00 |
| Staff Salary | 25.50 |
| Graduate Assistant Salary | 4,605.56 |
| Annuity | 144.00 |
| Social Security | 36.60 |
| Consummable Supplies | 1,211.80 |
| Overhead | 7,441.75 |
| Other Expense | 211.91 |
| | $19,677.12 |

# *MISSION*
# *of*
# *Rome Air Development Center*

*RADC plans and conducts research, exploratory and advanced development programs in command, control, and communications ($C^3$) activities, and in the $C^3$ areas of information sciences and intelligence. The principal technical mission areas are communications, electromagnetic guidance and control, surveillance of ground and aerospace objects, intelligence data collection and handling, information system technology, ionospheric propagation, solid state sciences, microwave physics and electronic reliability, maintainability and compatibility.*


Printed by
United States Air Force
Hanscom AFB, Mass. 01731